Eur. Phys. J. D **18**, 365–370 (2002)
DOI: 10.1140/epjd/e20020042

THE EUROPEAN PHYSICAL JOURNAL D
EDP Sciences

Photoionization and detection of ultracold Cs_2 molecules through diffuse bands

C.M. Dion[1], O. Dulieu[1,a], D. Comparat[1], W. de Souza Melo[1], N. Vanhaecke[1], P. Pillet[1], R. Beuc[2], S. Milošević[2], and G. Pichler[1,2]

[1] Laboratoire Aimé Cotton[b], CNRS, bâtiment 505, Campus d'Orsay, 91405 Orsay Cedex, France
[2] Institute of Physics, P.O. Box 304, 10001 Zagreb, Croatia

Received 13 September 2001

Abstract. We present the results of absorption measurements in a cesium vapor around 630 K, together with photoionization spectra through a resonance-enhanced two-photon absorption of ultracold cesium dimers created after photoassociation of ultracold cesium atoms. The maximum efficiency of the ultracold molecule ionization is found for wavelengths where absorption at thermal energies is the strongest, in agreement with our theoretical simulations of both processes, involving the so-called Cs_2 diffuse bands. This result will be helpful for further optimization of such a direct way of detection of ultracold molecules.

PACS. 33.80.Eh Autoionization, photoionization, and photodetachment – 33.80.Gj Diffuse spectra; predissociation, photodissociation – 33.80.Ps Optical cooling of molecules; trapping

1 Introduction

Since their first observation in 1997 [1], cold ($T \approx 0.01-1$ K) and ultracold molecules ($T < 0.001$ K) have encountered a growing interest from many research groups around the world, investigating several kinds of formation processes. Up to now, the photoassociation (PA) of a pair of ultracold atoms is the only way to produce molecular samples with temperatures lying in the microkelvin range (demonstrated for Cs_2 [1,2], K_2 [3,4], and Rb_2 [5]), or even in the nanokelvin range [6], as it overcomes the inherent difficulties of direct laser cooling of molecules [7]. During the PA process, a pair of ultracold atoms within a trap absorbs a photon with a frequency detuned to the red of an atomic resonance [8], in order to populate rovibrational levels of an attractive molecular potential, which then decay through spontaneous or stimulated emission to form stable ultracold molecules. Use of a number of non-optical methods to cool molecules to the 0.1–1 K temperature range has also been reported, such as buffer gas cooling techniques [9] or cooling with electrostatic forces [10]. Other alternative methods have also been proposed [11–13].

In all the above studies, the detection efficiency of the cold molecules is the keypoint for proving their existence. Up to now, the most efficient solution, in experiments investigating ultracold molecule formation through PA of ultracold atoms, consists in resonant two-photon ionization of the ultracold molecules into molecular ions, through the absorption into rovibrational levels of an intermediate excited molecular state [1]. Figure 1 shows the relevant states in the case of ultracold cesium molecules. Such a process, usually referred to as a REMPI (Resonance-Enhanced Multi-Photon Ionization) process, fulfills the sensitivity requirement for the direct — though destructive — detection of the usually small amount ($\sim 10^3 - 10^4$ for cesium) of ultracold molecules created. This method has already been helpful to generate high-resolution PA spectra of cesium [14,15] and rubidium [16] dimers, providing a wealth of spectroscopic data on long-range molecular states, elastic scattering properties, or radiative lifetimes.

At thermal energies, several studies have been devoted to the so-called diffuse bands in high-pressure alkali vapors [17,18], involving an absorption transition similar to the first step of the REMPI process described above. It is well-known [19] that such bands correspond to molecular transitions which are enhanced when the energy difference between the potential curves involved exhibits one or several extrema.

In this paper, we present experimental results showing that in the cesium case, the recorded absorption profile at thermal energies, is very surprisingly similar to the enveloppe of the molecular ion spectra observed in the ultracold experiment above. This implies also that the best ionization efficiency of ultracold molecules, *i.e.*, the largest ion signal, is found at the energy position of maxima in the absorption coefficient at thermal energies. We describe in detail in Section 2 both the absorption experiment performed at thermal energy and experimental results of the ionization of ultracold Cs_2 molecules. In Section 3, the theoretical interpretation of these results is given,

[a] e-mail: olivier.dulieu@lac.u-psud.fr
[b] Unité propre du CNRS 3321

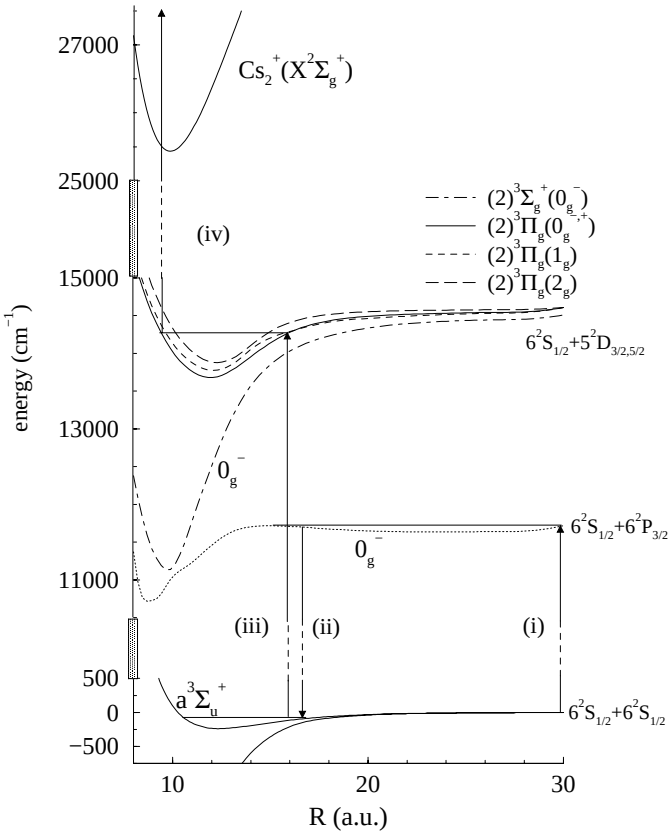

Fig. 1. Formation and detection of ultracold cesium molecules. (i) Photoassociation of a pair of ultracold ground state atoms into levels of the double-well 0_g^- state correlated to the 6S + 6P$_{3/2}$ asymptote. (ii) Spontaneous emission towards the lowest $a^3\Sigma_u^+$ state. (iii, iv) Two-photon ionization of ultracold Cs_2 molecules, through absorption into levels of the $(2)^3\Pi_g(0_g^{+,-}, 1_g, 2_g)$ fine-structure manifold or of the $(2)^3\Sigma_g^+(0_g^-)$ state, correlated to the 6S + 5D$_{5/2}$ asymptotes.

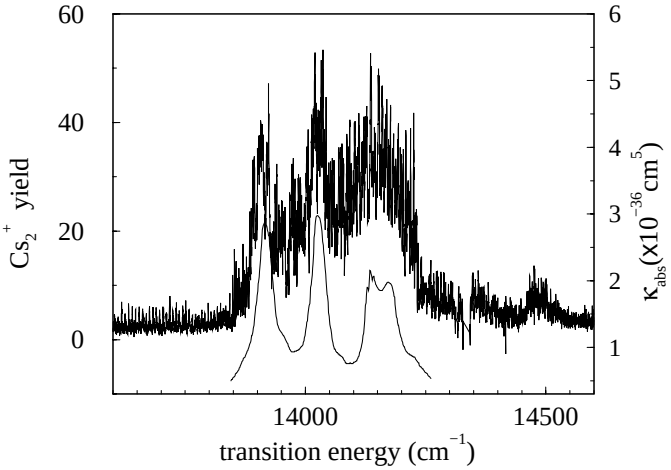

Fig. 2. The experimental reduced absorption coefficient $\kappa_{\rm abs}$ (lower trace) at $T = 620$ K, as a function of the transition energy; the upper trace shows the Cs_2^+ ion yield recorded during the photoassociation of the $0_g^-(P_{3/2})$ $v \approx 134$ level. The detuning of the PA laser is fixed at $\delta_{\rm PA} = 0.43$ cm^{-1}, while the pulsed laser wavelength $\lambda_{\rm ion}$ is scanned.

which involves the concept of difference potentials [19]. A semiclassical calculation of the absorption rate in the thermal regime, and a quantum modelling of the molecular ion signal recorded in the experiment, involving steps (i), (ii) and (iii) in Figure 1, are briefly described. Their results are discussed in detail and compared to experiment, and the role of step (iv) of this figure is examined in relation to other photionization experiments [20,21].

2 Experimental details

2.1 Absorption of a cesium vapor at thermal energies

We performed absorption measurements using a T-shaped pyrex glass cesium cell placed in two separately heated chamber ovens. The temperature of the lower cell part containing liquid cesium was kept at 605 K (defines vapor pressure). The temperature of the upper cell part of 12.8 cm in length could be varied up to 630 K. This gives a cesium atom density $n_{\rm Cs} = 6.35 \times 10^{16}$ cm^{-3}, which is suitable for a precise absorption measurement of diffuse Cs_2 molecular bands. The source of background radiation was a stabilized halogen lamp. The transmitted light was spectrally resolved by means of a monochromator (Jobin-Yvon 1 500, 2 400 grooves/mm), detected by a red-sensitive photomultiplier and recorded on a strip-chart recorder. The amount of absorption at diffuse band maxima was below 10%. In order to obtain the higher accuracy needed for the observation of numerous oscillations in the band profiles, we electronically compensated I_0, the lamp background intensity, and the difference in transmitance without and with cesium vapor in the cell were amplified. In Figures 2 and 3 we present the resulting cesium diffuse bands profiles represented uniquely by using the reduced absorption coefficient $\kappa_{\rm abs} = k/n_{\rm Cs}^2$, expressed in cm^5, where k is the absorption coefficient in cm^{-1}. It is interesting to note that the band has three distinct peaks. On the shorter wavelength side the peak is obviously formed of two overlapping bands, of which the one at 707 nm has on its top three smaller peaks [22].

2.2 Ionization spectrum of ultracold Cs_2 molecules

The details of the experimental setup for photoassociation of ultracold atoms in a Cs vapor-cell magneto-optical trap can be found in references [1,23]. The main characteristics of the trap are a temperature around 130 μK and a peak density of 10^{11} cm^{-3} for 5×10^7 atoms. The power of the PA laser can be tuned within the 50–500 W/cm^2, and is chosen at 100 W/cm^2 in the present experiment, yielding a rate for the production of ultracold molecules ranging within 0.1–0.2 molecules per second and per atom. The formation of ultracold molecules *via* photoassociation can be demonstrated by using a very sensitive REMPI detection (Fig. 1). In this article, the photoassociation step selects a rovibrational level for detunings $\delta_{\rm PA} = 0.43$ cm^{-1},

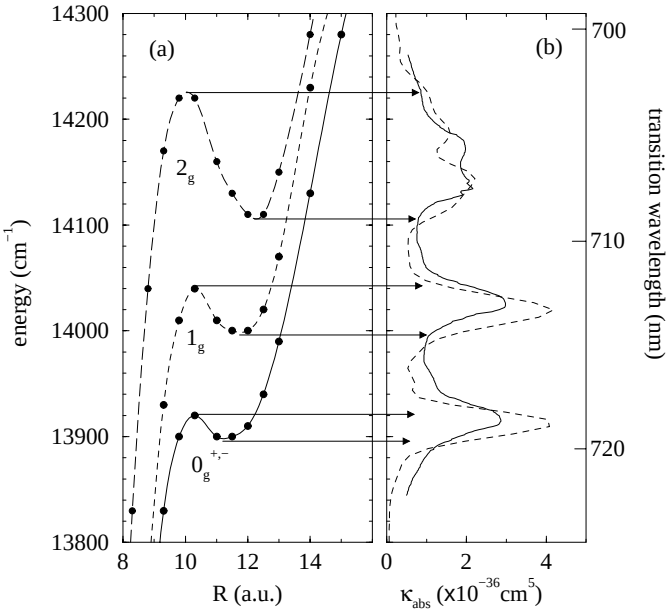

Fig. 3. (a) Difference potential curves for the $a^3\Sigma_u^+ - (2)^3\Pi_g(0_g^{+,-}, 1_g, 2_g)$ transition, relevant for the present diffuse band analysis. Quantum chemistry calculations from reference [26] are used. (b) Experimental (solid line) and calculated (dashed line) reduced absorption coefficient at $T = 630$ K. The calculated curve is shifted in order to match the amplitude of the 2_g peaks. Arrows suggest the correspondance between maxima in the absorption spectrum and extrema in the difference potentials.

16.06 cm^{-1}, and 70.28 cm^{-1} (corresponding to $v \approx 134$, $v = 55$, or $v = 4$, respectively), lying within the external well of the Cs_2 $0_g^-(6S + 6P_{3/2})$ double-well state [14] (step (i) in Fig. 1). Neglecting the atomic hyperfine structure, such levels decay spontaneously into a distribution of rovibrational levels of the lowest triplet state $a^3\Sigma_u^+$ (step (ii) in Fig. 1). These ultracold molecules are then ionized into Cs_2^+ ions by using a pulsed dye laser (7 ns duration, 1 mJ energy, focused to a 1 mm^2 spot, providing a power of about 10^7 W/cm^2) pumped by the second harmonic of a Nd–YAG laser, at a 10 Hz repetition rate (steps (iii) and (iv) in Fig. 1). Its wavelength λ_{ion} is scanned over the 685–735 nm range, as in the experiment at thermal energies.

The first photon of the REMPI process (step (iii) in Fig. 1) induces bound-bound absorption between $a^3\Sigma_u^+$ levels of the ultracold molecules and $(2)^3\Pi_g(0_g^{+,-}, 1_g, 2_g)$ or $(2)^3\Sigma_g^+(0_g^-)$ levels. The second step (step (iv) in Fig. 1) corresponds to a one-photon ionization of these intermediate levels.

After the photoionizing laser pulse, a strong, pulsed electric field (3 kV/cm, 0.5 μs) is applied at the trap position by means of a pair of grids spaced 15 mm apart to accelerate the ions. The ions expelled from the photoassociation region in a 6 cm free field zone constituting a time-of-flight mass spectrometer, in order to separate the Cs_2^+ ions from Cs^+ ions. A pair of microchannel plates detects the ions. This detection scheme is quite sensitive, allowing the detection of single ions. However, the global efficiency of such a detection is moderate: it is limited by the ion recollection rate (∼90%) and the microchannel plate efficiency (∼35%), while the REMPI efficiency is estimated of the order of 10%. By comparing the Cs_2^+ ion signal with the trap loss fluorescence signal, and using calculated branching ratio between bound-bound and bound-free absorption probabilities for the molecules [24,25], no more than 5% of the formed ultracold molecules are then detected. As shown in reference [25], this number can even vanish when ultracold molecules are formed into rovibrational levels very close to the dissociation limit of the triplet state: their radial wavefunction is concentrated at large distances (beyond $50a_0$), where the transition dipole moment is close to the $(6s \rightarrow 5d)$ atomic one, *i.e.*, equal to zero.

We reproduce in Figure 2 the Cs_2^+ ion yield recorded after photoassociation of the $0_g^-(P_{3/2})$ $v \approx 134$ level, at a detuning $\delta_{PA} = 12$ GHz. Within the 13 850–14 250 cm^{-1} transition energy range, a very dense spectrum is obtained, proving that almost all vibrational levels of the ultracold molecules in the $a^3\Sigma_u^+$ state can be excited towards $(2)^3\Pi_g$ levels when scanning the ionization laser [24]. The width of the pulsed laser (∼ 10 GHz) and field broadening effects (see Sect. 3) prevent a detailed spectroscopic analysis of such vibrational bands. The enveloppe of the present ion spectrum and of the reduced absorption coefficient at thermal energies presented above are very similar, suggesting that the same absorption step plays the main role in both cases. We discuss below the interpretation of these results in terms of difference potentials and absorption through diffuse bands of Cs_2.

3 Theoretical interpretation

The interpretation of the previous experimental spectra follows directly from the behavior of the difference potentials corresponding to the transition between the lowest triplet state $a^3\Sigma_u^+$ and the fine-structure manifold $(2)^3\Pi_g(0_g^{+,-}, 1_g, 2_g)$ (correlated to the $6S+5D_{5/2}$ dissociation limit), drawn in Figure 3a. They are deduced from the quantum chemistry calculations of reference [26] including spin-orbit interaction. As discussed in reference [19], when difference potentials exhibit one extremum or more, the transition probability, and then the absorption rate are expected to be enhanced at specific wavelength ranges, where the transition amplitude builds up through the constructive interference of multiple Condon points. For instance, in Figure 3a, three Condon points are present in the 703–709 nm range, between the two extrema of the $2_g - a^3\Sigma_u^+$ difference potential. Actually, all difference potential curves in Figure 3a exhibit one minimum and one maximum, with an increasing energy separation for the $0_g^{+,-} - a^3\Sigma_u^+$, $1_g - a^3\Sigma_u^+$, and $2_g - a^3\Sigma_u^+$ pairs, respectively. Local maxima observed in the experimental signal correspond to this effect, as demonstrated below.

In the following, effects due to the Cs hyperfine structure and the rotational coupling will be neglected.

3.1 Semiclassical determination of the absorption coefficient

Theoretical simulations of Cs_2 diffuse band absorption coefficient at $T = 630$ K are performed using the semiclassical approach already described in reference [27], and not recalled here, considering the interaction potential curves mentionned above. The correspondence shown with arrows in Figure 3 emphasizes the good agreement, obtained without any adjustment in the potential curves, between the wavelength range for multiple Condon points (at most three) in between extrema in difference potentials, and the location of peaks in the experimental absorption coefficient. This low resolution spectroscopy technique yields thus an estimate for the accuracy of computed difference potentials, of about 20 cm^{-1} here. Such a situation involving three Condon points has also been discussed in a previous study on Cs_2 cusp satellite bands [28]. As the calculations are performed in relative units, the magnitude of the 2_g peak has been matched to the experimental one. A small discrepancy still remains in the intensities of the $0_g^{+,-}$ and 1_g peaks, possibly due the transition dipole moment functions which actually differ in all components of the Cs_2 diffuse bands. The *ab initio* calculations of reference [26] give only one transition dipole moment function for Hund's case (a) $(2)^3\Pi_g$ potential. In our calculations we actually assumed that all transitions in question possess this same transition dipole function, which in reality might differ from component to component of the diffuse bands, due to a large spin-orbit coupling, and possible perturbations of other close-lying electronic states of the same symmetry.

3.2 Calculation of the number of ions produced by photoionization of ultracold molecules

We simulate the Cs_2^+ ion spectrum by calculating the number of molecular ions formed, $\mathcal{N}_{\rm ion}$, for a $0_g^-(P_{3/2})$ vibrational level detuned by $\delta_{\rm PA}$, analogously to the expression derived in reference [25],

$$\mathcal{N}_{\rm ion}(\delta_{\rm PA}) = \mathcal{N}_{\rm PA}(\delta_{\rm PA}) \sum_{v''} \mathcal{P}_{\rm ion}(v'') \left|\left\langle v(0_g^-)|v''(a^3\Sigma_u^+)\right\rangle\right|^2 \tag{1}$$

where the R-dependence of the dipole transition function for the spontaneous decay step has been neglected [24]. In this equation, $\mathcal{N}_{\rm PA}(\delta_{\rm PA})$ is the number of molecules accumulated during the PA step, which is obtained from

$$\mathcal{N}_{\rm PA}(\delta_{\rm PA}) = \mathcal{R}_{\rm PA}(\delta_{\rm PA}) t_{\rm PA} n_{\rm PA}, \tag{2}$$

with $\mathcal{R}_{\rm PA}(\delta_{\rm PA})$ the photoassociation rate of the $0_g^-(P_{3/2})$ vibrational level under consideration, whose expression has already been discussed in details in references [24,29], $t_{\rm PA} \simeq 10$ ms the residence time of the ultracold molecules in the trap area, and $n_{\rm PA} = 5 \times 10^6$ the number of atoms in the photoassociation area. The ionization probability $\mathcal{P}_{\rm ion}(v'')$ of the $a^3\Sigma_u^+$ vibrational levels v'' is estimated after assuming that the second step of the REMPI process is well described by a uniform ionization probability of the levels v' of the $(2)^3\Pi_g$ manifold [21], which is omitted in the following. We thus write

$$\mathcal{P}_{\rm ion}(v'') = \zeta \sum_{v'} \left|\left\langle v'((2)^3\Pi_g)\right| D \left|v''(a^3\Sigma_u^+)\right\rangle\right|^2 f(\nu_{v'',v'}), \tag{3}$$

with D the R-dependent $a^3\Sigma_u^+ \rightarrow (2)^3\Pi_g$ transition dipole moment [26], $f(\nu_{v'',v'}) = \exp\left[-c\left(\nu_{v'',v'} - \nu_{\rm ion}\right)^2\right]$ accounting for the resolution of the experiment, estimated at $\delta\nu \sim 30$ GHz, and ζ a constant ensuring that the probability is normalized to one [30]. In this expression, $c = \ln 2/\left(\delta\nu\right)^2$, $\nu_{v'',v'}$ is the frequency of the $v''(a^3\Sigma_u^+) \rightarrow v'((2)^3\Pi_g)$ transition, and $\nu_{\rm ion}$ is the frequency of the ionizing laser used in the experiment. As in reference [25], all bound state energies and wavefunctions and associated overlap integrals are computed using the mapped Fourier grid Hamiltonian method, which has been shown in previous work [31] to be well adapted to levels with very large elongation.

As quoted in the description of the experimental REMPI set-up, the pulsed ionizing laser has a pretty high intensity, which induces saturation effects in the absorption. The Franck-Condon-type hypothesis of equation (1) is then probably not well adapted to the representation of line intensities in the experimental ion spectrum of Figure 4. A crude estimation of this effect consists in replacing equation (1) by

$$\mathcal{N}_{\rm ion}(\delta_{\rm PA}) = \sum_{v''} \min\left(S, \mathcal{N}_{\rm PA}(\delta_{\rm PA}) \mathcal{P}_{\rm ion}(v'') \left|\left\langle v(0_g^-)|v''(a^3\Sigma_u^+)\right\rangle\right|^2\right), \tag{4}$$

where S is an upper limit for number of ions formed from a given v'' level. After several trials, the value for S is fixed at 450, which provides a good agreement of the computed rate with the experimental one, as shown in Figure 4a for $v \approx 134$. The similar overall modulation of both types of curves is still visible for the two other cases $v = 55$ and $v = 4$ displayed in Figures 4b and 4c, with a contrast in the computed signal more pronounced than in the experimental one. It may be due to an inaccurate S value, as PA levels are producing various vibrational distributions [24] with probably different saturation patterns. However we can see that at least for the two levels $v = 134$ and 55 (Figs. 4a and 4b) the ratio of the number of ions produced is the same in the experiment and in the model. Better agreement could be obtained by an experimental determination of the factor ζ used in equation (3) and a more precise treatment of saturation effects. Furthermore, the deeper the PA level is in the 0_g^- external well, the closer to the dissociation limit are the populated levels in the lowest triplet state of the ultracold molecules [24]. Hyperfine interaction within the 6S + 6S manifold should be invoked, bringing the possibility to create ultracold molecules in the $X^1\Sigma_g^+$ ground state, which is not included as a decay channel in the present treatment. A detailed study of these issues is under progress.

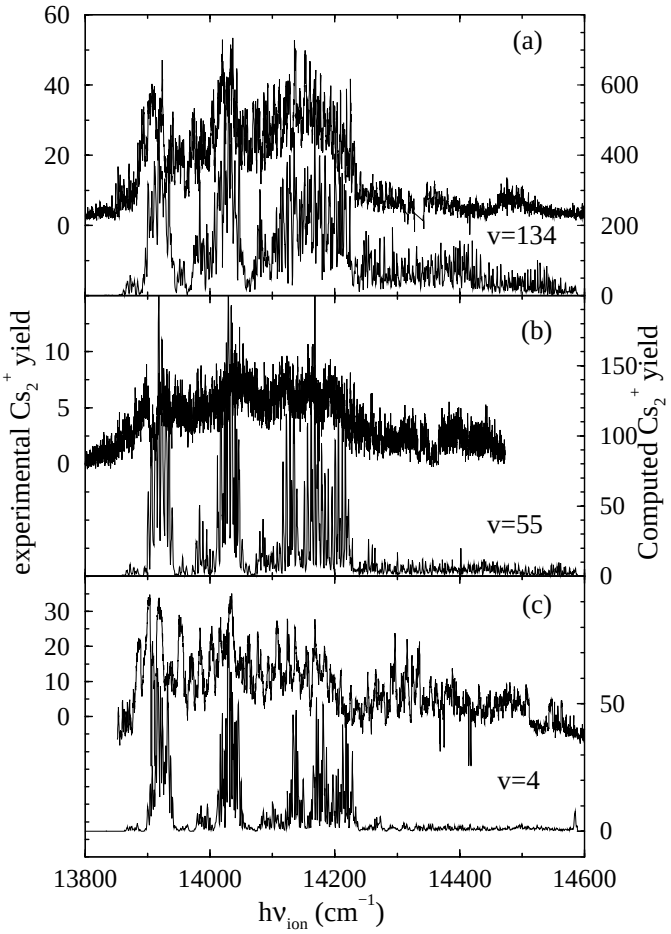

Fig. 4. Recorded ion yield (upper traces, left vertical scale) and computed Cs_2^+ number $\mathcal{N}_{\rm ion}$ (lower traces, right vertical scale) as functions of the ionizing laser wavelength $\lambda_{\rm ion}$, for photoassociation of various $0_g^-(P_{3/2})$ vibrational levels: (a) $v = 134$, or $\delta_{\rm PA} = 0.43$ cm^{-1}, (b) $v = 55$, or $\delta_{\rm PA} = 16.06$ cm^{-1}, (c) $v = 4$, or $\delta_{\rm PA} = 70.28$ cm^{-1}. The saturation parameter (see text) is fixed in the simulation to 450. Notice the similar reduction in both vertical scales from (a) to (c).

The good agreement between the absorption coefficient and the enveloppe of the ion signal can be easily understood. The experiment at thermal energies relies on the free-bound transition (or photoassociation) from a pair of ground state hot atoms towards the $(2)^3\Pi_g$ manifold. The Maxwell distribution of energies washes out all stuctures in the resulting spectrum. The ion yield recorded after the ionization of ultracold molecules results from bound-bound transitions between the same electronic states. In both cases, the transitions are controlled by the same set of difference potentials, which determine the position of maxima in the absorption spectrum. This result also confirms that the second step of the REMPI process, *i.e.* the transition into the Cs_2 electronic continuum, does not influence the shape of the spectrum [21].

Below 13 850 cm^{-1}, regularly spaced lines with weaker intensity are also visible (see Fig. 2, upper trace). In addition to very weak lines associated to the $(2)^3\Pi_g$ manifold (the bottom of the $0_g^{+,-}$ well lies slightly below 13 700 cm^{-1}), they result from the ionization through the $(2)^3\Sigma_g^+(0_g^-)$ state (drawn in Fig. 1), for which the difference potential with $a^3\Sigma_u^+$ has no extremum over the wavelength range investigated here. This state represents another possible ionization step, yielding a much simpler spectrum, as it has no fine structure (see also Ref. [16]). These lines are completly hidden in the domain of the above diffuse bands. Beyond 14 250 cm^{-1}, both $(2)^3\Sigma_g^+$ and $(2)^3\Pi_g$ contribute simultaneously with comparable magnitude, again giving rise to a very dense spectrum.

Finally, one can comment on the order of magnitude difference in the absolute magnitude of the computed ion number shown in Figure 4 with the experimental signal, which is already quite satisfactory, given the hypothesis of our model. First the experimental conditions reported in Section 2.2, linked to the ion recollection and microchannel plate efficiency, lower the experimental signal by a factor 3 to 4. The computed signal results from a balance between overestimation, due to the assumed uniform ionization probability (actually taken equal to 1) for the second ionization step, and underestimation due to our crude saturation model, and to the absence of some possible channels involved in the whole process of ultracold molecule formation and detection. Given all these hypothesis, the magnitude of the computed signal should then be considered as satisfactory.

4 Conclusion

In this work, we investigated the properties of the detection scheme of ultracold cesium molecules, based on resonance-enhanced two-photon ionization. It represents a very efficient and sensitive detection method, which is now well understood through the link with standard absorption measurements of a cesium vapor at room temperatures. The maximum efficiency of the ultracold molecule ionization is found for laser wavelengths around 716 nm, where maxima of the absorption signal (or diffuse bands) are observed. According to our theoretical simulations, such maxima are due to the occurence of multiple Condon points in the related difference potentials. Experimental results are given in the case of ultracold cesium molecules created in their lowest triplet state $a^3\Sigma_u^+$, after spontaneous decay of molecules excited in the long-range $0_g^-(6S + 6P_{3/2})$ state by photoassociation of ultracold atoms. Theoretical simulations show that ionization proceeds mainly through the intermediate $(2)^3\Pi_g(0_g^-, 0_g^+, 1_g, 2_g)(6S + 5D_{5/2})$ excited states, also responsible for the diffuse bands observed in absorption experiment at thermal energies. A good agreement between theory and experiment is obtained for ultracold molecules yielded by the decay of the $0_g^-(6S + 6P_{3/2})$ uppermost vibrational levels, as the final $a^3\Sigma_u^+$ vibrational distribution is spread over a large part of the potential well. In contrast, the agreement is less satisfactory for deeper $0_g^-(6S + 6P_{3/2})$ levels, which produce ultracold molecules in vibrational levels close to the dissociation limit,

in a region where hyperfine structure strongly mixes both $a^3\Sigma_u^+$ and $X^1\Sigma_g^+$ states.

Similar studies should then be performed for other ultracold molecule experiment. For example, photoassociation of cesium molecules in ungerade states (the long-range $1_u(6S + 6P_{3/2})$ state [15], or the $0_u^+(6S + 6P_{1/2})$ [25]) will mainly produce ultracold molecules in their ground state $X^1\Sigma_g^+$. It should also be noted that recent absorption experiments have detected another diffuse band around 543.5 nm in cesium, attributed to the $a^3\Sigma_u^+ \rightarrow (3)\Pi_g(6S + 7P_{3/2})$ [27], providing another probable efficient path for ultracold molecule detection, as already mentionned in reference [1].

Contributions from B. Laburthe Tolra, C. Drag and A. Fioretti are gratefully acknowledged. G.P. thanks the hospitality of Laboratoire Aimé Cotton during a 3-month visit supported by CNRS. This work was partially supported by the Ministry of Science and Technology, Croatia, under contracts number 0350101 and 0350102, and by NSERC Canada (to C.M.D.). Calculations of ultracold molecule formation have been performed on vectorial computers at IDRIS (Orsay, France).

References

1. A. Fioretti, D. Comparat, A. Crubellier, O. Dulieu, F. Masnou-Seeuws, P. Pillet, Phys. Rev. Lett. **80**, 4402 (1998).
2. T. Takekoshi, B.M. Patterson, R.J. Knize, Phys. Rev. Lett. **81**, 5105 (1998).
3. A.N. Nikolov, E.E. Eyler, X.T. Wang, J. Li, H. Wang, W.C. Stwalley, P.L. Gould, Phys. Rev. Lett. **82**, 703 (1999).
4. A.N. Nikolov, J.R. Enscher, E.E. Eyler, H. Wang, W.C. Stwalley, P.L. Gould, Phys. Rev. Lett. **84**, 246 (2000).
5. C. Gabbanini, A. Fioretti, A. Lucchesini, S. Gozzini, M. Mazzoni, Phys. Rev. Lett. **84**, 2814 (2000).
6. R. Wynar, R.S. Freeland, D.J. Han, C. Ryu, D.J. Heinzen, Science **287**, 1016 (2000).
7. J.T. Bahns, P.L. Gould, W.C. Stwalley, J. Chem. Phys. **104**, 9689 (1996).
8. H.R. Thorsheim, J. Weiner, P.S. Julienne, Phys. Rev. Lett. **58**, 2420 (1987).
9. R. deCarvalho, J.M. Doyle, B. Friedrich, T. Guillet, J. Kim, D. Patterson, J.D. Weinstein, Eur. Phys. J. D **7**, 289 (1999).
10. H.L. Bethlem, G. Berden, G. Meijer, Phys. Rev. Lett. **83**, 1558 (1999).
11. J.A. Maddi, T.P. Dineen, H. Gould, Phys. Rev. A **60**, 3882 (1999).
12. M. Gupta, D. Herschbach, J. Phys. Chem. A **103**, 10670 (1999).
13. V. Vuletič, S. Chu, Phys. Rev. Lett. **84**, 17 (2000).
14. A. Fioretti, D. Comparat, C. Drag, C. Amiot, O. Dulieu, F. Masnou-Seeuws, P. Pillet, Eur. Phys. J. D **5**, 389 (1999).
15. D. Comparat, C. Drag, B. Laburthe Tolra, A. Fioretti, P. Pillet, A. Crubellier, O. Dulieu, F. Masnou-Seeuws, Eur. Phys. J. D **11**, 59 (2000).
16. A. Fioretti, C. Amiot, C.M. Dion, O. Dulieu, M. Mazzoni, G. Smirne, C. Gabbanini, Eur. Phys. J. D **15**, 189 (2001).
17. G. Pichler, S. Milošević, D. Veža, R. Beuc, J. Phys. B: At. Mol. Opt. Phys. **16**, 4619 (1983).
18. W.T. Luh, J.T. Bahns, A.M. Lyyra, K.M. Sando, P.D. Kleiber, W. Stwalley, J. Chem. Phys. **88**, 2235 (1988).
19. J. Tellinghuisen, in *Photodissociation and Photoionization*, edited by K.P. Lawley (Wiley, New York, 1985).
20. H. Suemitsu, S. Imai, E. Yoshida, H. Imanishi, I. Naba, J. Phys. Soc. Jap. **59**, 1981 (1990).
21. H. Suemitsu, H. Kitaura, K. Seki, J. Phys. Soc. Jap. **62**, 3425 (1993).
22. U. Diemer, J. Gress, W. Demtröder, Chem. Phys. Lett. **178**, 330 (1991).
23. D. Comparat, C. Drag, A. Fioretti, O. Dulieu, P. Pillet, J. Mol. Spectrosc. **195**, 229 (1999).
24. C. Drag, B. Laburthe Tolra, O. Dulieu, D. Comparat, M. Vatasescu, S. Boussen, S. Guibal, A. Crubellier, P. Pillet, IEEE J. Quant. Electron. **36**, 1378 (2000).
25. C.M. Dion, C. Drag, O. Dulieu, B. Laburthe Tolra, F. Masnou-Seeuws, P. Pillet, Phys. Rev. Lett. **86**, 2253 (2001).
26. N. Spiess, Ph.D. thesis, Universität Kaiserslautern, 1989.
27. T. Ban, H. Skenderović, R. Beuc, G. Pichler, Europhys. Lett. **48**, 378 (1999).
28. D. Veža, R. Beuc, S. Milošević, G. Pichler, Eur. Phys. J. D **2**, 45 (1998).
29. P. Pillet, A. Crubellier, A. Bleton, O. Dulieu, P. Nosbaum, I. Mourachko, F. Masnou-Seeuws, J. Phys. B: At. Mol. Opt. Phys. **30**, 2801 (1997).
30. This constant is deduced from the observation that the calculated $\mathcal{P}_{\rm ion}$ saturates as v'' decreases to 0 as can be seen in Figure 4 of reference [25]. ζ is chosen as a maximal value such that $\mathcal{P}_{\rm ion}(v''=0)=1$.
31. V. Kokoouline, O. Dulieu, R. Kosloff, F. Masnou-Seeuws, J. Chem. Phys. **110**, 9865 (1999).